Inorganic Chemistry

Article

pubs.acs.org/IC

2D Cd(II)−Lanthanide(III) Heterometallic−Organic Frameworks Based on Metalloligands for Tunable Luminescence and Highly Selective, Sensitive, and Recyclable Detection of Nitrobenzene

Shu-Ran Zhang,[†] Dong-Ying Du,[†] Jun-Sheng Qin,[†] Shun-Li Li,[‡] Wen-Wen He,[†] Ya-Qian Lan,*[,‡] and Zhong-Min Su*[,†]

[†]Institute of Functional Material Chemistry, Faculty of Chemistry, Northeast Normal University, Changchun, 130024, Jilin, People's Republic of China

[‡]Jiangsu Key Laboratory of Biofunctional Materials, School of Chemistry and Materials Science, Nanjing Normal University, Nanjing, 210023, Jiangsu, People's Republic of China

Supporting Information

ABSTRACT: In this work, five novel 2D isostructural Cd(II)−lanthanide(III) heterometallic−organic frameworks $[CdCl(L)Eu_xTb_y(H_2O)(DMA)](NO_3)\cdot 3DMA$ (**IFMC-36-Eu$_x$Tb$_y$**: $x = 1$, $y = 0$, **IFMC-36-Eu**; $x = 0.6$, $y = 0.4$, **IFMC-36-Eu$_{0.6}$Tb$_{0.4}$**; $x = 0.5$, $y = 0.5$, **IFMC-36-Eu$_{0.5}$Tb$_{0.5}$**; $x = 0.4$, $y = 0.6$, **IFMC-36-Eu$_{0.4}$Tb$_{0.6}$**; $x = 0$, $y = 1$, **IFMC-36-Tb**; H_3L is 4,4′,4″-((2,2′,2″-(nitrilotris(methylene))tris(1*H*-benzo[*d*]-imidazole-2,1-diyl))tris(methylene))tribenzoic acid; IFMC = Institute of Functional Material Chemistry) have been successfully synthesized by taking advantage of different molar ratios of lanthanide(III) (Ln(III)) and metalloligands under solvothermal conditions. Further luminescent measurements indicate that **IFMC-36-Eu$_x$Tb$_y$** exhibits characteristic sharp emission bands of Eu(III) and Tb(III), and the intensities of red and green can be modulated correspondingly by tuning the ratios of Eu(III) and Tb(III). Particularly, the solvent-dependent luminescent behavior of **IFMC-36-Eu** shows a potential application in detection of small-molecule pollutant nitrobenzene by significant fluorescence quenching. Furthermore, **IFMC-36-Eu** displays preeminent anti-interference ability and could be used for sensing in the systems with complicated components. This is the first time that a d−f heterometallic−organic framework can be investigated as a chemical sensor for selective, sensitive, and recyclable detection of nitrobenzene.

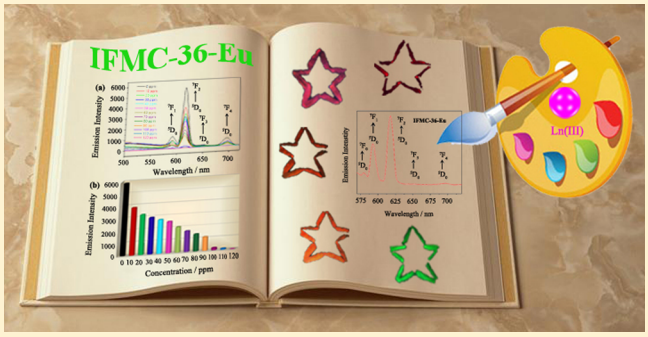

INTRODUCTION

Metal−organic frameworks (MOFs) have been an active research field and receiving considerable attention from both academia and industry not merely because of diverse topologies with aesthetic beauty, but also for their potential applications in numerous areas.[1] MOFs as extremely promising multifunctional luminescent materials have been the focus of significant interest, and a great deal of effort has been devoted to this domain.[2] It may be due to the inherent advantages of MOFs as single metal cations (primary building unit or PBU) or metal clusters (secondary building unit or SBU) and organic linkers,[3] as well as the tailorability in MOFs, including but not limited to structure, dimension, size, and shape.[4] In general, the metal components can contribute to photoluminescence; on this occasion, Ln(III)[5] or various inorganic clusters[6] are often involved. Furthermore, the organic ligands with aromatic moieties or conjugated π systems are in a position to give rise to optical emission or photoluminescence upon excitation.[7] Among these various kinds of luminescent MOFs, lanthanide-(III) metal−organic frameworks (LnMOFs) are of particular interest due to their unique high luminescence quantum yield, narrow bandwidth, notable fluorescence monochromaticity, characteristic sharp emission in the visible region, long excited-state luminescence lifetimes (up to milliseconds), and large Stokes shift (>200 nm).[8] It is noteworthy that the research in d−f heterometallic−organic frameworks is rapidly expanding.[9] In general, Ln(III) luminescent materials can be classified into two categories: (1) Ln(III) ions coordinated directly to the organic linkers/sensitizers[10] and (2) Ln(III) ions encapsulated into porous MOFs.[11] However, it still remains a significant challenge for rational "design" and "control" of tailor-made LnMOFs with expected structures and applications in synthesis chemistry and materials science by virtue of high coordination numbers of typically more than six and variable nature of the Ln(III) sphere.[12]

Nowadays, instead of pure organic linkers in the construction of traditional MOFs, metalloligands as metal-containing complexes with the coordination binding sites are widely utilized to further coordinate/bind with the second metal ions

Received: May 13, 2014
Published: July 23, 2014

   dx.doi.org/10.1021/ic5011083 | *Inorg. Chem.* 2014, 53, 8105−8113

and/or metal clusters.[13] As highlighted recently, metalloligands have the following advantages over traditional organic ligands. (1) Metalloligands are typically longer and more flexible, which are very appealing to design and construct MOFs with diverse topologies and aesthetic beauty.[14] (2) Next is the straightforward immobilization of functional sites, including metal and organic functional sites, such as open metal sites, catalytically active metal sites, photoactive metal sites, and magnetic sites,[15] which leads one to target some multifunctional MOFs materials. (3) Moreover, metalloligands with extra coordination sites (carboxylate, nitrile, and pyridyl groups) are ideal candidates for the construction of MOFs through self-assembly and stepwise synthesis.[16] To the best of our knowledge, Ln(III) ions have a high affinity and prefer O to N donors, whereas the 3d metal ions have a tendency to coordinate with both N and O donors.[17] Thus, the coordination sites, such as carboxylate groups and nitrogen atoms, can be correspondingly coordinated by Ln(III) ions and transition metals. Furthermore, Ln(III) ions suffer from weak light absorption due to the forbidden f → f transitions (Laporte forbidden), which can be solved by a ligand-to-metal energy transfer (also known as an "antenna effect").[18] This can result in effective lanthanide luminescence, and yet is dependent on the energetic position of the relevant singlet and triplet states of the coordination compounds.[19] On the other hand, trivalent lanthanide metal cations like Eu(III) and Tb(III) as fascinating luminescent sources have attracted more attention due to high color purity, fluorescent efficiency, and extreme sensitivity to the coordination environments.[20] As stated above, it is a novel and available synthetic strategy to obtain LnMOFs in the combination of metalloligands and Ln(III) ions. It is apparent that the research on metalloligands for functional LnMOFs is still at the early stage.

Up to now, a variety of LnMOFs have been successfully constructed for potential applications in chemical sensing,[21] light-emitting devices,[22] proton conductors,[23] bioresponsive imaging,[24] and so on.[25] Nonetheless, for various applications, fluorescence detection based on chemical sensing has proven to be an excellent candidate for the rapid recognition and sensing of cations, anions, small molecules, and vapors.[26] Fluorescence-based detection possesses these advantages of high sensibility, simplicity, short response time, and the ability to be applied in both solution and solid phase as compared to traditional detection methods. A wide range of LnMOFs as chemical sensors have been investigated and reported by Chen, Harbuzaru, Liu, and co-workers.[27] Moreover, chemical sensors for the detection of nitroaromatics explosive-like substances are of high importance concerning homeland security, environmental, and humanitarian implications.[28] Among various nitroaromatics, nitrobenzene as a simple nitro-containing compound is the basic and the simplest constituent of nitroaromatic explosives. Likewise, nitrobenzene is also a highly toxic and notorious environmental pollutant that can give rise to serious health problems.[29] Therefore, it is an extremely urgent issue to explore an effective method for recyclable probe for the sensitive detection of nitrobenzene by taking environmental and safety problems into consideration. In previous work, we have constructed an extremely stable Cd(II) MOF for highly selective detection of nitroaromatic explosives based on H_3L (4,4′,4″-((2,2′,2″-(nitrilotris(methylene))tris(1*H*-benzo[*d*]imidazole-2,1-diyl))tris(methylene))tribenzoic acid).[30] As a continuation and improvement of our work, we took advantage of H_3L as metalloligands and obtained a series of tunable luminescent 2D Cd(II)−Ln(III) heterometallic−organic frameworks $[CdCl(L)Eu_xTb_y(H_2O)(DMA)](NO_3)\cdot 3DMA$ (**IFMC-36-Eu$_x$Tb$_y$**: $x = 1$, $y = 0$, **IFMC-36-Eu**; $x = 0.6$, $y = 0.4$, **IFMC-36-Eu$_{0.6}$Tb$_{0.4}$**; $x = 0.5$, $y = 0.5$, **IFMC-36-Eu$_{0.5}$Tb$_{0.5}$**; $x = 0.4$, $y = 0.6$, **IFMC-36-Eu$_{0.4}$Tb$_{0.6}$**; $x = 0$, $y = 1$, **IFMC-36-Tb**). **IFMC-36-Eu$_x$Tb$_y$** emits characteristic red and green colors of Eu(III) and Tb(III) ions, respectively. Notably, **IFMC-36-Eu** displays high selectivity, sensitivity, and recyclability toward detecting nitrobenzene in solution at ppm level, which might be used for a fluorescent sensor nitrobenzene sensing application through a photoinduced electron-transfer (PET) mechanism. This is the first report on a d−f heterometallic−organic framework that displays highly selective, sensitive, and recyclable properties in the detection of nitrobenzene as a fluorescent sensor. However, it is still a labor-intensive endeavor to synthesize new families of LnMOF materials for highly selective and recyclable detection of nitroaromatic explosives.

EXPERIMENTAL SECTION

Materials and Instrumentation. Chemicals were obtained from commercial sources and were used without further purification. Powder X-ray diffraction (PXRD) was performed on a Siemens D5005 diffractometer with Cu Kα (λ = 1.5418 Å) radiation in the range of 3−60° at 293 K. Elemental microanalyses (C, H, and N) were performed on a PerkinElmer 240C elemental analyzer; Eu and Tb were determined with an ICP-OES spectrometer (U.S.). Before carrying out elemental analyses, we precisely weighed a certain quantity of the crystals, then dissolved the sample into the HNO_3 aqueous solution (1:1) and fixed the volume to 25 mL. Finally, we tested the corresponding component concentration in the solution by ICP analysis. IR spectra were recorded in the range 4000−400 cm^{-1} on an Alpha Centaurt FT/IR spectrophotometer using KBr pellets. Thermogravimetric analysis (TGA) was performed on a PerkinElmer TG-7 analyzer heated from 50 to 1000 °C at a ramp rate of 10 °C min^{-1} under nitrogen. Solid-state fluorescence spectra for the compounds were recorded on an F-4600 FL spectrophotometer equipped with a xenon lamp and quartz carrier at room temperature. The excited-state lifetime was measured on a transient spectrofluorimeter (Edinburgh FLS920) with a time-correlated single-photocounting technique.

Synthesis of $[CdCl(L)Eu(H_2O)(DMA)](NO_3)\cdot 3DMA$ (IFMC-36-Eu). A mixture of H_3L (0.03 g, 0.04 mmol), $Cd(NO_3)_2\cdot 4H_2O$ (0.16 g, 0.52 mmol), $Eu(NO_3)_3\cdot 6H_2O$ (0.08 g, 0.18 mmol), DMA (5 mL), H_2O (3 mL), and four drops of HCl (6 mol L^{-1}) was sealed in a Teflon-lined stainless steel container and heated in an autoclave at 100 °C for 4 days. After the autoclave was cooled to room temperature, light yellow crystals were obtained and isolated by washing with DMA and dried at room temperature. Yield: 62% based on H_3L. Anal. Calcd for $C_{64}H_{73}N_{12}O_{14}ClCdEu$: C, 50.10; H, 4.81; N, 10.96; Eu, 9.90. Found: C, 50.03; H, 4.88; N, 11.05; Eu, 9.85. IR (cm^{-1}, Supporting Information Figure S1a): 3422 (s), 2941 (m), 1625 (s), 1546 (m), 1492 (m), 1453 (s), 1421 (s), 1403 (s), 1188 (m), 1019 (m), 956 (w), 893 (w), 755 (w), 595 (w), 474 (w).

Synthesis of $[CdCl(L)Eu_{0.6}Tb_{0.4}(H_2O)(DMA)](NO_3)\cdot 3DMA$ (IFMC-36-Eu$_{0.6}$Tb$_{0.4}$). **IFMC-36-Eu$_{0.6}$Tb$_{0.4}$** was synthesized by a procedure similar to that used for **IFMC-36-Eu** with $Eu(NO_3)_3\cdot 6H_2O$ (0.05 g, 0.11 mmol) and $Tb(NO_3)_3\cdot 6H_2O$ (0.03 g, 0.07 mmol) instead of $Eu(NO_3)_3\cdot 6H_2O$ (0.08 g, 0.18 mmol). The light yellow crystals were isolated by washing with DMA and dried at room temperature. Yield: 58% based on H_3L. Anal. Calcd for $C_{64}H_{73}N_{12}O_{14}ClCdEu_{0.6}Tb_{0.4}$: C, 50.01; H, 4.80; N, 10.94; Eu, 5.93; Tb, 4.14. Found: C, 49.96; H, 4.89; N, 11.03; Eu, 5.87; Tb, 4.17. IR (cm^{-1}, Supporting Information Figure S1b): 3427 (s), 2935 (m), 1621 (s), 1545 (s), 1485 (s), 1184 (m), 1018 (m), 958 (w), 920 (w), 862 (w), 759 (s), 722 (m), 642 (w), 596 (m), 475 (w), 421 (m).

Synthesis of $[CdCl(L)Eu_{0.5}Tb_{0.5}(H_2O)(DMA)](NO_3)\cdot 3DMA$ (IFMC-36-Eu$_{0.5}$Tb$_{0.5}$). **IFMC-36-Eu$_{0.5}$Tb$_{0.5}$** was synthesized by a procedure similar to that used for **IFMC-36-Eu** with $Eu(NO_3)_3\cdot 6H_2O$

dx.doi.org/10.1021/ic5011083 | *Inorg. Chem.* 2014, 53, 8105−8113

(0.04g, 0.09 mmol) and $Tb(NO_3)_3·6H_2O$ (0.04 g, 0.09 mmol) instead of $Eu(NO_3)_3·6H_2O$ (0.08 g, 0.18 mmol). The light yellow crystals were isolated by washing with DMA and dried at room temperature. Yield: 60% based on H_3L. Anal. Calcd for $C_{64}H_{73}N_{12}O_{14}ClCdEu_{0.5}Tb_{0.5}$: C, 49.98; H, 4.79; N, 10.93; Eu, 4.94; Tb, 5.17. Found: C, 40.92; H, 4.84; N, 11.01; Eu, 4.88; Tb, 5.11. IR (cm^{-1}, Supporting Information Figure S1c): 3430 (s), 2935 (m), 1619 (s), 1546 (s), 1338 (s), 1184 (m), 1018 (m), 958 (w), 862 (w), 759 (s), 722 (w), 642 (w), 596 (m), 475 (w), 422 (m).

Synthesis of $[CdCl(L)Eu_{0.4}Tb_{0.6}(H_2O)(DMA)](NO_3)·3DMA$ (IFMC-36-$Eu_{0.4}Tb_{0.6}$). **IFMC-36-$Eu_{0.4}Tb_{0.6}$** was synthesized by a procedure similar to that used for **IFMC-36-Eu** with $Eu(NO_3)_3·6H_2O$ (0.03g, 0.07 mmol) and $Tb(NO_3)_3·6H_2O$ (0.05 g, 0.11 mmol) instead of $Eu(NO_3)_3·6H_2O$ (0.08 g, 0.18 mmol). The light yellow crystals were isolated by washing with DMA and dried at room temperature. Yield: 57% based on H_3L. Anal. Calcd for $C_{64}H_{73}N_{12}O_{14}ClCdEu_{0.4}Tb_{0.6}$: C, 49.96; H, 4.79; N, 10.93; Eu, 3.95; Tb, 6.20. Found: C, 49.88; H, 4.86; N, 11.02; Eu, 3.89; Tb, 6.08. IR (cm^{-1}, Supporting Information Figure S1d): 3430 (s), 2935 (m), 1620 (s), 1546 (s), 1338 (s), 1184 (m), 1018 (m), 958 (w), 862 (w), 759 (s), 722 (w), 642 (w), 596 (m), 475 (w), 422 (m).

Synthesis of $[CdCl(L)Tb(H_2O)(DMA)](NO_3)·3DMA$ (IFMC-36-Tb). **IFMC-36-Tb** was synthesized by a procedure similar to that used for **IFMC-36-Eu** with $Tb(NO_3)_3·6H_2O$ (0.08g, 0.18 mmol) instead of $Eu(NO_3)_3·6H_2O$ (0.08 g, 0.18 mmol). The light yellow crystals were isolated by washing with DMA and dried at room temperature. Yield: 63% based on H_3L. Anal. Calcd for $C_{64}H_{73}N_{12}O_{14}ClCdTb$: C, 49.87; H, 4.78; N, 10.91; Tb, 10.31. Found: C, 49.81; H, 4.87; N, 11.02; Tb, 10.25. IR (cm^{-1}, Supporting Information Figure S1e): 3425 (s), 2940 (m), 1626 (s), 1546 (s), 1492 (s), 1342 (s), 1184 (m), 1019 (m), 957 (w), 866 (w), 755 (m), 723 (w), 647 (w), 595 (m), 474 (w).

X-ray Crystallography. Single-crystal X-ray diffraction data in this work were recorded on a Bruker APEXII CCD diffractometer with graphite-monochromated Mo K_α radiation (λ = 0.71069 Å) at 293 K. Absorption corrections were applied using multiscan technique. All of the structures were solved by Direct Method of SHELXS-97[31a] and refined by full-matrix least-squares techniques using the SHELXL-97 program[31b] within WINGX.[31c] Non-hydrogen atoms were refined with anisotropic temperature parameters. The SQUEEZE program implemented in PLATON was used to remove these electron densities for the compounds. Thus, all of the electron densities from free solvent molecules have been "squeezed" out. The detailed crystallographic data and structure refinement parameters are summarized in Supporting Information Table S1.

RESULTS AND DISCUSSION

When combining the ligand H_3L with $Cd(NO_3)_2·4H_2O$ and different molar ratios of $Eu(NO_3)_3·6H_2O$ and $Tb(NO_3)_3·6H_2O$, **IFMC-36-Eu_xTb_y** has been obtained. Single-crystal X-ray diffraction studies reveal that **IFMC-36-Eu_xTb_y** crystallizes in the triclinic space group $P\bar{1}$ (Supporting Information Table S1) and is isostructural only with slight differences in bond lengths and bond angles. Therefore, only the structure of **IFMC-36-Eu** is described in detail. The crystallographically independent unit contains a Cd^{2+} ion, a Eu^{3+} ion, a Cl^- ion, an L^{3-} ion, a NO^{3-} ion, three DMA molecules, and a H_2O molecule. The coordination environments of the Cd atom and Eu atom are presented in Figure 1a. The Cd atom coordinates to four nitrogen atoms from the same L^{3-} ligand and a chlorine atom from HCl (Cd–N, 2.256–2.583 Å and Cd–Cl, 2.426 Å, Supporting Information Table S2). Eu1 is nine-coordinated by seven carboxylate oxygen atoms from four H_3L ligands, one oxygen atom from DMA, and one from water molecule (Eu–O, 2.379–2.685 Å and Eu–O1w, 2.480 Å), which generates a binuclear europium cluster $[Eu_2(CO_2)_6(DMA)_2(H_2O)_2]$ (Supporting Information Figure S2). The Eu–O bond lengths are all within the normal ranges as reported in the literature.[32] One

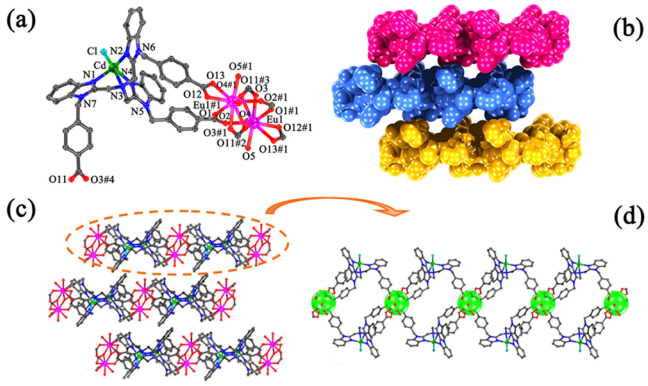

Figure 1. (a) Coordination environments of Cd(II) and Eu(III) in **IFMC-36-Eu**. Symmetry code: #1 $-x + 1, -y + 1, -z$; #2 $-x, -y + 2, -z$; #3 $x + 1, y - 1, z$; #4 $x - 1, y + 1, z$. (b) Space-filling representation of **IFMC-36-Eu**. (c and d) Ball-and-stick representations of its packing arrangement of the 2D sheet-like structure in **IFMC-36-Eu**, respectively. All of the hydrogen atoms are omitted for clarity.

L^{3-} anion coordinates to four Eu(III) cations and two binuclear europium clusters; in turn, one binuclear europium cluster connects four L^{3-} ions (Supporting Information Figure S3). Further study into the nature of this architecture reveals that **IFMC-36-Eu** displays a two-dimensional network in the *ab* plane (Figure 1c and d). Figure 1b shows the space-filling representation of **IFMC-36-Eu**. The integrities of **IFMC-36-Eu_xTb_y** were confirmed by powder X-ray diffraction (PXRD) (Supporting Information Figure S4). The diffraction peaks of both simulated and as-synthesized patterns match well in key positions, thus indicating their phase purities. The thermal behaviors of **IFMC-36-Eu_xTb_y** were studied by thermogravimetric analysis (TGA, Supporting Information Figure S5a–e).

The application of metalloligands is a novel synthetic strategy in the construction of LnMOFs. We have also constructed d–f heterometallic–organic framework **IFMC-26-Eu_xTb_y** series based on metalloligands formed by H_4L under solvothermal conditions.[33] Although we obtained **IFMC-36-Eu_xTb_y** and **IFMC-26-Eu_xTb_y** in similar conditions, they made a big difference in crystallographic structure, as **IFMC-36-Eu_xTb_y** displays a 2D sheet-like structure, whereas **IFMC-26-Eu_xTb_y** exhibits a (3,6)-connected net with microporous structure (Scheme 1). The distinct coordination environment of Ln(III) ions and metalloligands may bring about the above-mentioned phenomenon. On the one hand, the result also shows that multicarboxylate ligands act as multifunctional organic ligands, which play important roles in the design of new LnMOFs.[34]

Scheme 1. Schematic Illustration for the Synthesis Routes and Topological Structures of IFMC-36-Eu and IFMC-26-Eu

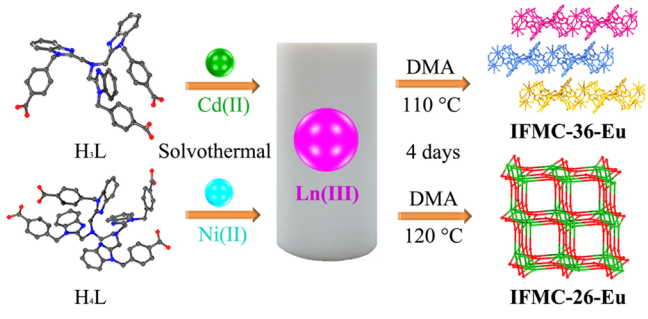

dx.doi.org/10.1021/ic5011083 | Inorg. Chem. 2014, 53, 8105–8113

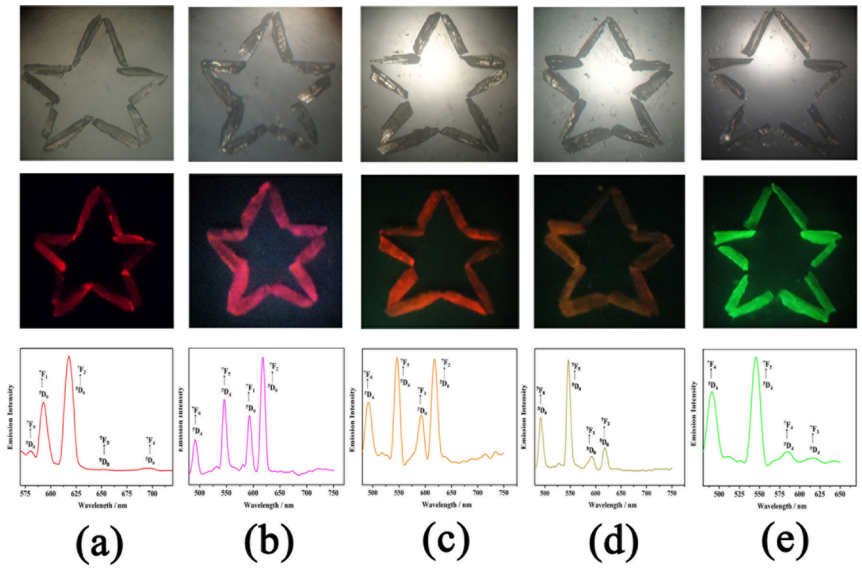

Figure 2. Photographs of **IFMC-36-Eu$_x$Tb$_y$** (under natural light and laboratory UV light (365 nm)), and emission spectra of (a) **IFMC-36-Eu** (red), (b) **IFMC-36-Eu$_{0.6}$Tb$_{0.4}$** (light red), (c) **IFMC-36-Eu$_{0.5}$Tb$_{0.5}$** (orange), (d) **IFMC-36-Eu$_{0.4}$Tb$_{0.6}$** (light yellow), and (e) **IFMC-36-Tb** (green).

Tetrapodand (H_4L) and tripodand (H_3L) can show various coordination modes to metal ions, resulting in the large diversity in the topologies. Tetrapodands may be more likely to form a 3D net with porous structures than tripodands due to carboxylate groups. On the other hand, by the force of contrast, it is obvious that different ligands respectively select the particular metals as the center in the formation of metal-loligands. In this regard, selecting the appropriate ligand and the metal ions is of much importance in the construction of LnMOFs based on metalloligands.

It is widely acknowledged that LnMOFs are gaining outstanding attention because of the advantages of the designability, which allow fine-tuned luminescence properties.[35] Therefore, luminescent properties of **IFMC-36-Eu$_x$Tb$_y$** in the solid state were investigated at room temperature. Upon excitation at 396 nm, **IFMC-36-Eu** yields narrow and characteristic peaks at 580, 593, 618, 652, and 697 nm due to $^5D_0 \rightarrow {}^7F_J$ (J = 0−4) transitions of the Eu(III) ion (Figure 2a). Among them, the most intense emission is attributed to the $^5D_0 \rightarrow {}^7F_2$ transition as an induced electric dipole transition, which is very sensitive to the coordination environment and responsible for the brilliant red emission.[36] Because the corresponding $^5D_0 \rightarrow {}^7F_1$ transition is a magnetic transition, the intensity of the emission band at 593 nm is relatively weak and fairly insensitive to the coordination environment. The $^5D_0 \rightarrow {}^7F_2$ transition is clearly stronger than that of $^5D_0 \rightarrow {}^7F_1$ with an intensity ratio of about 1.64 for $I(^5D_0 \rightarrow {}^7F_2)/I(^5D_0 \rightarrow {}^7F_1)$, suggesting that the coordination of Eu(III) does not exist in any inversion center in a local site. Because the $^5D_0 \rightarrow {}^7F_0$ and $^5D_0 \rightarrow {}^7F_1$ transitions are forbidden both in magnetic and in electric dipole schemes, their corresponding emission bands around 580 and 652 nm are very weak. **IFMC-36-Tb** yields an intense green luminescence when excited at 367 nm, which is assigned to the characteristic transitions of $^5D_4 \rightarrow {}^7F_J$ (J = 6−3) of Tb(III) ion. Two intense emission bands at 491 and 546 nm correspond to the $^5D_4 \rightarrow {}^7F_6$ and $^5D_4 \rightarrow {}^7F_5$ transitions, while the weaker emission bands at 584 and 617 nm originate from $^5D_4 \rightarrow {}^7F_4$ and $^5D_4 \rightarrow {}^7F_3$, respectively (Figure 2e). **IFMC-36-Eu$_x$Tb$_y$** (x = 0.6, y = 0.4, **IFMC-36-Eu$_{0.6}$Tb$_{0.4}$**; x = 0.5, y = 0.5, **IFMC-36-Eu$_{0.5}$Tb$_{0.5}$**; x = 0.4, y = 0.6, **IFMC-36-Eu$_{0.4}$Tb$_{0.6}$**) were successfully prepared through tuning the ratios of Eu(III):Tb(III). The various ratios of Eu(III) and Tb(III) in **IFMC-36-Eu$_x$Tb$_y$** show different emission intensities, in which the emission bands at 593 and 618 nm are relative to the $^5D_0 \rightarrow {}^7F_1$ and $^5D_0 \rightarrow {}^7F_2$ transitions of Eu(III) and the other two at 584 and 617 nm are attributed to the transitions of $^5D_4 \rightarrow {}^7F_6$ and $^5D_4 \rightarrow {}^7F_5$ of Tb(III), respectively (Figure 2b−d). The Eu(III) and Tb(III) emitted their respective red and green colors upon excitation with a standard UV lamp (λ_{ex} = 365 nm), which can be readily observed by the naked eye. The optical images were displayed by using a fluorescence microscope equipped with a CCD camera (Figure 2). As we expected, the intensities of red and green arising from Eu(III) and Tb(III) emissions can be shifted correspondingly. The excitation and emission spectra were also recorded under similar conditions (Supporting Information Figure S6).

The decay curve of transition $^5D_0 \rightarrow {}^7F_2$ (618 nm) for **IFMC-36-Eu** is well-fitted by exponential function, yielding the lifetime value of τ = 0.64 ms (Supporting Information Figure S7a). Similarly, for **IFMC-36-Tb**, the decay curve of transitions $^5D_4 \rightarrow {}^7F_5$ (546 nm) is well-fitted by exponential function, yielding the lifetime value of τ = 1.11 ms (Supporting Information Figure S7b). Moreover, both the Eu(III) and the Tb(III) decay curves in **IFMC-36-Eu$_{0.6}$Tb$_{0.4}$**, **IFMC-36-Eu$_{0.5}$Tb$_{0.5}$**, and **IFMC-36-Eu$_{0.4}$Tb$_{0.6}$** were also monitored (Supporting Information Figure S7). The Eu(III) and Tb(III) decay curves respectively detected at 618 and 546 nm of **IFMC-36-Eu$_{0.6}$Tb$_{0.4}$**, **IFMC-36-Eu$_{0.5}$Tb$_{0.5}$**, and **IFMC-36-Eu$_{0.4}$Tb$_{0.6}$** are also well-fitted by exponential functions. The changes in lifetime of different Ln(III) ions in **IFMC-36-Eu$_x$Tb$_y$** may be ascribed to their environments. Meanwhile, we have also presented corresponding lifetime values and quantum yields of **IFMC-36-Eu$_x$Tb$_y$** (Supporting Information Table S3). It is worthwhile to note that **IFMC-36-Eu$_x$Tb$_y$** have much more obvious luminescent intensity, longer excited-state lifetime, and higher quantum yield than those of the **IFMC-26-Eu$_x$Tb$_y$** series (Supporting Information Table S4), which may be assumed due to the following two reasons. (1) As far as we know, the fine-tuning of light-emitting properties of these LnMOF materials is the identical coordination environment of

dx.doi.org/10.1021/ic5011083 | Inorg. Chem. 2014, 53, 8105−8113

the different Ln(III) ions. The dissimilar chemical reactivity and coordination behavior of Ln(III) ions in these two series may result from the different metalloligands we have adopted. (2) On the other hand, the different centers of metalloligands, Cd(II) and Ni(II), respectively, usually show high complexation affinity to carboxylate and varied coordination numbers and geometries. However, Cd(II) scarcely interferes with fluorescence as compared to Ni(II), thus giving rise to different luminescent behavior in different LnMOFs. Hitherto, studies on tunable luminescence properties based on LnMOFs are still in their infancy in fluorescent materials science.

The fascinating optical properties of LnMOFs inspire us to carefully explore their potential applications. The luminescence spectrum of the **IFMC-36-Eu** sample dispersed in DMA is shown in Figure 3a. It exhibits characteristic electronic

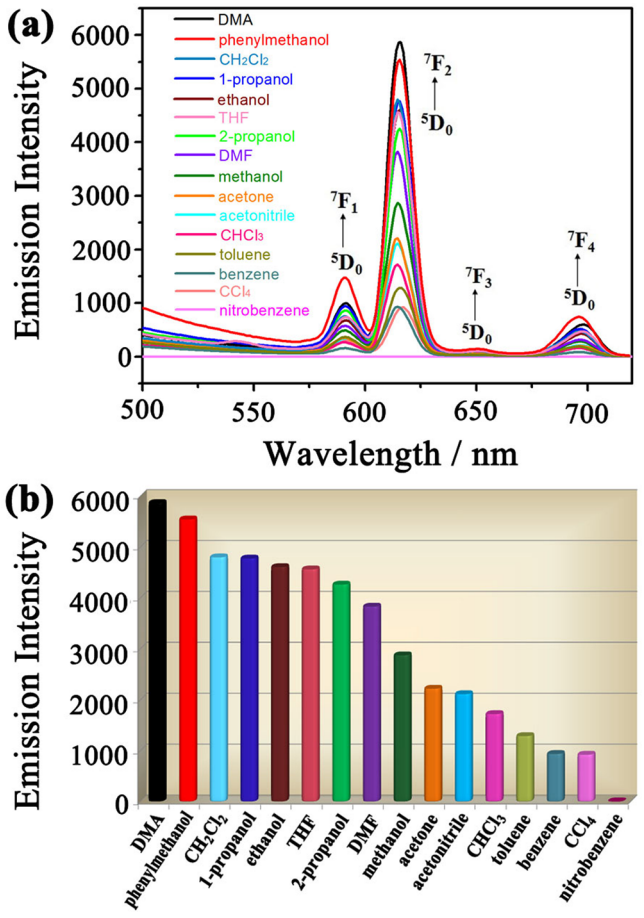

Figure 3. (a) Emission spectra and (b) the $^5D_0 \rightarrow {}^7F_2$ transition intensities of **IFMC-36-Eu** introduced into various pure solvents when excited at 367 nm.

transitions of Eu(III) at 593, 617, 651, and 699 nm upon excitation at 367 nm, which are attributed to the $^5D_0 \rightarrow {}^7F_1$, $^5D_0 \rightarrow {}^7F_2$, $^5D_0 \rightarrow {}^7F_3$, and $^5D_0 \rightarrow {}^7F_4$, respectively. It is obvious that the $^5D_0 \rightarrow {}^7F_2$ transition is clearly stronger than that of $^5D_0 \rightarrow {}^7F_1$ with an intensity ratio of about 5.9 for $I(^5D_0 \rightarrow {}^7F_2)/I(^5D_0 \rightarrow {}^7F_1)$. The characteristic bright-red luminescence of **IFMC-36-Eu** primarily prompts us to investigate its potential for sensing common organic solvent molecules. To examine the potential of **IFMC-36-Eu** toward sensing of small molecules, the fluorescence properties of **IFMC-36-Eu** in different solvent emulsions were investigated (Figure 3a). The finely ground sample of **IFMC-36-Eu** (3 mg) was immersed in 3 mL of different organic solvents, treated by ultrasonication for 30 min, and then aged for 3 h to form stable suspensions before the fluorescence study. The solvents used are methanol, ethanol, 1-propanol, 2-propanol, phenylmethanol, tetrahydrofuran (THF), *N*,*N*-dimethylformamide (DMF), acetone, acetonitrile, dichloromethane (CH_2Cl_2), chloroform ($CHCl_3$), carbon tetrachloride (CCl_4), toluene, benzene, and nitrobenzene. The framework of **IFMC-36-Eu** is intact after immersion in different solvents as confirmed by PXRD (Supporting Information Figure S8). The most intriguing feature was that the photoluminescence (PL) intensity of $^5D_0 \rightarrow {}^7F_2$ transition at 617 nm of Eu(III) is largely dependent on the solvent molecules (Figure 3b), in which the physical interaction between the solute and solvent plays a vital role.

Notably, the PL intensity exhibits significant quenching behaviors especially in the case of nitrobenzene. Therefore, such solvent-dependent quenching behavior is appropriate for the detection of nitrobenzene. To examine the sensitivity of sensing nitrobenzene in more detail, a batch of suspensions of **IFMC-36-Eu** was dispersed in DMA solution, while the nitrobenzene content was gradually increased to monitor the emissive response (Figure 4a). The luminescence intensity of the **IFMC-36-Eu** suspension significantly decreases into 55.7% at a nitrobenzene concentration of only 50 ppm, and almost

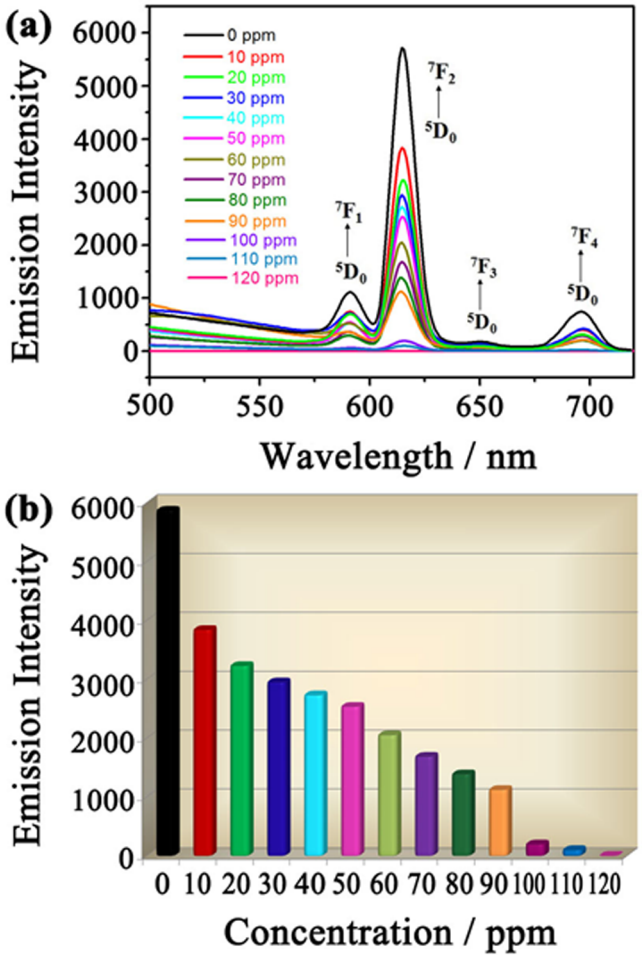

Figure 4. (a) Emission spectra and (b) the $^5D_0 \rightarrow {}^7F_2$ transition intensities of **IFMC-36-Eu** introduced into different concentrations of nitrobenzene in DMA (excited at 367 nm).

dx.doi.org/10.1021/ic5011083 | *Inorg. Chem.* 2014, 53, 8105−8113

completely quenches at 120 ppm (Figure 4b). **IFMC-36-Eu** displays a higher sensitivity than those of other MOFs in sensing nitrobenzene.[37] That is probably largely because of the combined action of Cd(II) and Ln(III) ions. Besides the high selectivity of **IFMC-36-Eu** toward nitrobenzene, the organic solvent on the anti-interference ability of the sensor is vitally important. We have tested the PL spectra of **IFMC-36-Eu** dispersed in DMA with the addition of different 4000 ppm organic solvents (Supporting Information Figure S9) and subsequent addition of 120 ppm nitrobenzene (Supporting Information Figure S10). The interferences of other organics on the fluorescence response of **IFMC-36-Eu** to nitrobenzene were nearly unperturbed even when there is a great deal of other organics (4000 ppm) in the system with nitrobenzene (120 ppm, Figure 5). The fluorescence intensity ratio at the $^5D_0$

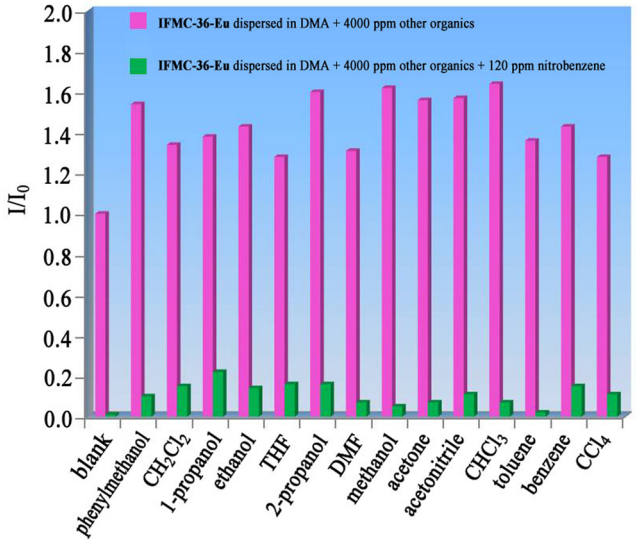

Figure 5. Fluorescence intensity ratio (I/I_0) histograms of **IFMC-36-Eu** dispersed in DMA with the addition of different 4000 ppm organic solvents (pink) and subsequent addition of 120 ppm nitrobenzene (green). Emission intensities at the $^5D_0 \rightarrow {}^7F_2$ transition were selected.

$\rightarrow {}^7F_2$ transition was calculated by the formula (I/I_0), in which I is the fluorescence intensity of **IFMC-36-Eu** after adding other organics and I_0 is the fluorescence intensity of **IFMC-36-Eu** dispersed in DMA. Apparently, the fluorescence intensities of the suspension were remarkably decreased with the subsequent addition of 120 ppm nitrobenzene into the parallel tests. Additionally, we also found that **IFMC-36-Eu** can be regenerated and reused for a significant number of cycles by centrifugation of the solution after use and washing several times with DMA.[38] The quenching efficiencies of every cycle are basically unchanged at about 55% (Figure 6) through monitoring the emission spectra of **IFMC-36-Eu** dispersed in the presence of 50 ppm nitrobenzene in DMA from cycle 1 to 8 (Supporting Information Figure S11). The quenching efficiency (%) was estimated using the formula $(I_0 - I)/I_0 \times 100\%$, where I_0 and I are the $^5D_0 \rightarrow {}^7F_2$ transition intensities of **IFMC-36-Eu** before and after exposure to 50 ppm nitrobenzene in DMA, respectively. The PXRD pattern further confirms that the framework is retained after cycle 8 (Supporting Information Figure S12). These results reveal that **IFMC-36-Eu** shows outstanding anti-interference ability and could be applied as a fluorescence sensor for nitrobenzene with high sensitivity, selectivity, and recyclability in the systems with complicated

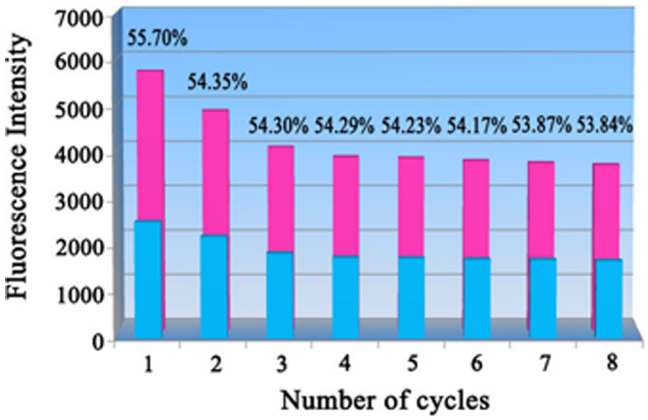

Figure 6. Reproducibility of the quenching ability of **IFMC-36-Eu** dispersed in DMA and in the presence of 50 ppm nitrobenzene. The pink bars represent the initial $^5D_0 \rightarrow {}^7F_2$ transition intensities, and the blue bars represent the intensities upon addition of a solution of 50 ppm nitrobenzene in DMA. The percentages on the top represent the quenching efficiency of every cycle.

components. As a result, **IFMC-36-Eu** can act as an excellent candidate for its sensitivity and recyclability in the field of detection application. The differences in quenching efficiency can be quantitatively treated with the Stern–Volmer (SV) equation: $(I_0/I) = K_{sv}[A] + 1$, in which I_0 is the initial fluorescence intensity without analyte, I represents the fluorescence intensity with added analyte of the molar concentration [A], and K_{sv} is the quenching constant (M^{-1}). A linear SV relationship for nitrobenzene is observed at low concentrations, but the plots subsequently deviate from linearity at higher concentrations (Supporting Information Figure S13). The nonlinear nature of the plot of the analytes may be ascribed to self-absorption or an energy-transfer process.[39] Therefore, the static and dynamic quenching may be coexisting and competitive in the fluorescence quenching process, which results in a nonlinear SV relationship. Fluorescence decays of **IFMC-36-Eu** at different concentrations of nitrobenzene also verify this (Supporting Information Figure S14). The excellent fluorescence quenching response to nitrobenzene can be attributed to the photoinduced electron-transfer mechanism. The finely ground powder of **IFMC-36-Eu** can be dispersed well in the solution, which would enable nitrobenzene to be closely adhered to the surface of the MOF particles and facilitate possible host–guest interactions.[40] The electron transfer from the electron-donating framework with rich π-electron to the highly electron-deficient nitrobenzene molecule adsorbed on the surface of the MOF particles can take place upon excitation, resulting in fluorescence quenching.

CONCLUSIONS

In summary, a series of heterometallic Ln-based tunable luminescent crystalline materials **IFMC-36-Eu$_x$Tb$_y$** based on metalloligands has been obtained by changing the molar ratios of Eu(III) and Tb(III). **IFMC-36-Eu$_x$Tb$_y$** not only exhibits the characteristic Eu(III) and Tb(III) emissions, but also multicolor emissions can be adjusted ranging from red to green by simply tuning their ratios. Especially, **IFMC-36-Eu** can display distinct solvent-dependent PL emissions and detect nitrobenzene with high selectivity, sensitivity, recyclability, and outstanding anti-interference ability through noticeable fluorescence quenching,

dx.doi.org/10.1021/ic5011083 | Inorg. Chem. 2014, 53, 8105–8113

which makes it an efficient and promising sensory material for trace nitrobenzene detection in an environmentally friendly manner. For the first time, a d−f heterometallic−organic framework can be utilized as a fluorescent sensor to detect nitrobenzene in the systems with complicated components. The fluorescence quenching mechanism is in consequence of photoinduced electron transfer from electron-rich LnMOF framework to electron-withdrawing nitrobenzene as well as the good dispersible nature of LnMOFs in these analytes. This work opens a promising approach to design multifunctional luminescent LnMOF by the combination of metalloligands and Ln(III). Considering the charming coordination ability between the diverse organic linkers and metallic elements, many look forward to synthesizing and exploring luminescent LnMOFs for various applications.

■ ASSOCIATED CONTENT

Supporting Information

Crystallographic data (CIF), PXRD, TGA, solid-state fluorescence decay curves of compounds, IR spectra, additional figures, and PL spectra. This material is available free of charge via the Internet at http://pubs.acs.org.

■ AUTHOR INFORMATION

Corresponding Authors

*E-mail: yqlan@njnu.edu.cn.
*E-mail: zmsu@nenu.edu.cn.

Notes

The authors declare no competing financial interest.

■ ACKNOWLEDGMENTS

This work was financially supported by Pre-973 Program (2010CB635114), the National Natural Science Foundation of China (nos. 21001020 and 21371099), the Jiangsu Specially Appointed Professor, the NSF of Jiangsu Province of China (no. BK20130043), the Natural Science Research of Jiangsu Higher Education Institutions of China (no. 13KJB150021), the Priority Academic Program Development of Jiangsu Higher Education Institutions, and the Foundation of Jiangsu Collaborative Innovation Center of Biomedical Functional Materials.

■ REFERENCES

(1) (a) Zhou, H.-C.; Long, J. R.; Yaghi, O. M. *Chem. Rev.* **2012**, *112*, 673−674. (b) Furukawa, H.; Cordova, K. E.; O'Keeffe, M.; Yaghi, O. M. *Science* **2013**, *341*, 1230444. (c) Kuppler, R. J.; Timmons, D. J.; Fang, Q.-R.; Li, J.-R.; Makal, T. A.; Young, M. D.; Yuan, D.; Zhao, D.; Zhuang, W.; Zhou, H.-C. *Coord. Chem. Rev.* **2009**, *253*, 3042−3066. (d) Long, J. R.; Yaghi, O. M. *Chem. Soc. Rev.* **2009**, *38*, 1213−1214. (e) Zhu, Q.-L.; Xu, Q. *Chem. Soc. Rev.* DOI: 10.1039/c3cs60472a. (f) Li, S.-L.; Xu, Q. *Energy Environ. Sci.* **2013**, *6*, 1656−1683. (g) Jiang, H.-L.; Feng, D.; Wang, K.; Gu, Z.-Y.; Wei, Z.; Chen, Y.-P.; Zhou, H.-C. *J. Am. Chem. Soc.* **2013**, *135*, 13934−13938. (h) Qin, J.-S.; Du, D.-Y.; Li, W.-L.; Zhang, J.-P.; Li, S.-L.; Su, Z.-M.; Wang, X.-L.; Xu, Q.; Shao, K.-Z.; Lan, Y.-Q. *Chem. Sci.* **2012**, *3*, 2114−2118.

(2) (a) Kreno, L. E.; Leong, K.; Farha, O. K.; Allendorf, M.; Duyne, R. P. V.; Hupp, J. T. *Chem. Rev.* **2012**, *112*, 1105−1125. (b) Guo, Z.; Xu, H.; Su, S.; Cai, J.; Dang, S.; Xiang, S.; Qian, G.; Zhang, H.; O'Keeffed, M.; Chen, B. *Chem. Commun.* **2011**, *47*, 5551−5553. (c) Decadt, R.; Hecke, K. V.; Depla, D.; Leus, K.; Weinberger, D.; Driessche, I. V.; Voort, P. V. D.; Deun, R. V. *Inorg. Chem.* **2012**, *51*, 11623−11634.

(3) (a) Lu, W.; Wei, Z.; Gu, Z.-Y.; Liu, T.-F.; Park, J.; Park, J.; Tian, J.; Zhang, M.; Zhang, Q.; Gentle, T., III; Bosch, M.; Zhou, H.-C. *Chem. Soc. Rev.* DOI: 10.1039/c4cs00003j. (b) Tranchemontagne, D. J.; Mendoza-Cortés, J. L.; O'Keeffe, M.; Yaghi, O. M. *Chem. Soc. Rev.* **2009**, *38*, 1257−1283. (c) Paz, F. A. A.; Klinowski, J.; Vilela, S. M. F.; Tomé, J. P. C.; Cavaleiro, J. A. S.; Rocha, J. *Chem. Soc. Rev.* **2012**, *41*, 1088−1110. (d) Dong, M.-J.; Zhao, M.; Ou, S.; Zou, C.; Wu, C.-D. *Angew. Chem., Int. Ed.* **2014**, *53*, 1575−1579.

(4) (a) Cui, Y.; Yue, Y.; Qian, G.; Chen, B. *Chem. Rev.* **2012**, *112*, 1126−1162. (b) Allendorf, M. D.; Bauer, C. A.; Bhakta, R. K.; Houk, R. J. T. *Chem. Soc. Rev.* **2009**, *38*, 1330−1352. (c) Chen, B.; Xiang, S.; Qian, G. *Acc. Chem. Res.* **2010**, *43*, 1115−1124.

(5) (a) Rocha, J.; Carlos, L. D.; Paz, F. A. A.; Ananias, D. *Chem. Soc. Rev.* **2011**, *40*, 926−940. (b) Liu, Y.; Pan, M.; Yang, Q.-Y.; Fu, L.; Li, K.; Wei, S.-C.; Su, C.-Y. *Chem. Mater.* **2012**, *24*, 1954−1960. (c) Zhang, Y.-H.; Li, X.; Song, S. *Chem. Commun.* **2013**, *49*, 10397−10399.

(6) (a) Kang, Y.; Wang, F.; Zhang, J.; Bu, X. *J. Am. Chem. Soc.* **2012**, *134*, 17881−17884. (b) Shan, X.-C.; Jiang, F.-L.; Yuan, D.-Q.; Zhang, H.-B.; Wu, M.-Y.; Chen, L.; Wei, J.; Zhang, S.-Q.; Pan, J.; Hong, M.-C. *Chem. Sci.* **2013**, *4*, 1484−1489. (c) Zhan, S.-Z.; Li, M.; Zhou, X.-P.; Ni, J.; Huang, X.-C.; Li, D. *Inorg. Chem.* **2011**, *50*, 8879−8892. (d) Knorr, M.; Guyon, F.; Khatyr, A.; Strohmann, C.; Allain, M.; Aly, S. M.; Lapprand, A.; Fortin, D.; Harvey, P. D. *Inorg. Chem.* **2012**, *51*, 9917−9934.

(7) Hu, Z.; Deibert, B. J.; Li, J. *Chem. Soc. Rev.* DOI: 10.1039/c4cs00010b.

(8) (a) Armelao, L.; Quici, S.; Barigelletti, F.; Accorsi, G.; Bottaro, G.; Cavazzini, M.; Tondello, E. *Coord. Chem. Rev.* **2010**, *254*, 487−505. (b) Eliseeva, S. V.; Bünzli, J. G. *Chem. Soc. Rev.* **2010**, *39*, 189−227.

(9) (a) Ward, M. D. *Coord. Chem. Rev.* **2007**, *251*, 1663−1677. (b) Yang, X.; Schipper, D.; Jones, R. A.; Lytwak, L. A.; Holliday, B. J.; Huang, S. *J. Am. Chem. Soc.* **2013**, *135*, 8468−8471. (c) Chandler, B. D.; Cramb, D. T.; Shimizu, G. K. H. *J. Am. Chem. Soc.* **2006**, *128*, 10403−10412. (d) Coppo, P.; Duati, M.; Kozhevnikov, V. N.; Hofstraat, J. W.; Cola, L. D. *Angew. Chem., Int. Ed.* **2005**, *44*, 1806−1810. (e) Biradha, K.; Su, C.-Y.; Vittal, J. J. *Cryst. Growth Des.* **2011**, *11*, 875−886.

(10) (a) Harbuzaru, B. V.; Corma, A.; Rey, F.; Jordá, J. L.; Ananias, D.; Carlos, L. D.; Rocha, J. *Angew. Chem., Int. Ed.* **2009**, *48*, 6476−6479. (b) Cui, Y.; Xu, H.; Yue, Y.; Guo, Z.; Yu, J.; Chen, Z.; Gao, J.; Yang, Y.; Qian, G.; Chen, B. *J. Am. Chem. Soc.* **2012**, *134*, 3979−3982. (c) Gai, Y.-L.; Jiang, F.-L.; Chen, L.; Bu, Y.; Su, K.-Z.; Al-Thabaiti, S. A.; Hong, M.-C. *Inorg. Chem.* **2013**, *52*, 7658−7665.

(11) (a) An, J.; Shade, C. M.; Chengelis-Czegan, D. A.; Petoud, S.; Rosi, N. L. *J. Am. Chem. Soc.* **2011**, *133*, 1220−1223. (b) Lan, Y.-Q.; Jiang, H.-L.; Li, S.-L.; Xu, Q. *Adv. Mater.* **2011**, *23*, 5015−5020. (c) Sava, D. F.; Rohwer, L. E. S.; Rodriguez, M. A.; Nenoff, T. M. *J. Am. Chem. Soc.* **2012**, *134*, 3983−3986. (d) Wei, Y.; Li, Q.; Sa, R.; Wu, K. *Chem. Commun.* **2014**, *50*, 1820−1823. (e) Luo, F.; Batten, S. R. *Dalton Trans.* **2010**, *39*, 4485−4488.

(12) (a) Zhou, Y.; Yan, B. *Inorg. Chem.* **2014**, *53*, 3456−3463. (b) Ji, M.; Lan, X.; Han, Z.; Hao, C.; Qiu, J. *Inorg. Chem.* **2012**, *51*, 12389−12394. (c) Roy, S.; Chakraborty, A.; Maji, T. K. *Coord. Chem. Rev.* **2014**, *273*, 139−164.

(13) (a) Kitagawa, S.; Kitaura, R.; Noro, S. *Angew. Chem., Int. Ed.* **2004**, *43*, 2334−2375. (b) Kosal, M. E.; Chou, J.-H.; Wilson, S. R.; Suslick, K. S. *Nat. Mater.* **2002**, *1*, 118−121.

(14) Das, M. C.; Guo, Q.; He, Y.; Kim, J.; Zhao, C.-G.; Hong, K.; Xiang, S.; Zhang, Z.; Thomas, K. M.; Krishna, R.; Chen, B. *J. Am. Chem. Soc.* **2012**, *134*, 8703−8710.

(15) (a) Das, M. C.; Xiang, S.; Zhang, Z.; Chen, B. *Angew. Chem., Int. Ed.* **2011**, *50*, 10510−10520. (b) Halper, S. R.; Do, L.; Stork, J. R.; Cohen, S. M. *J. Am. Chem. Soc.* **2006**, *128*, 15255−15268.

(16) (a) Suslick, K. S.; Bhyrappa, P.; Chou, J.-H.; Kosal, M. E.; Nakagaki, S.; Smithenry, D. W.; Wilson, S. R. *Acc. Chem. Res.* **2005**, *38*, 283−291. (b) Kitaura, R.; Onoyama, G.; Sakamoto, H.; Matsuda, R.; Noro, S.; Kitagawa, S. *Angew. Chem., Int. Ed.* **2004**, *43*, 2684−2687. (c) Smithenry, D. W.; Wilson, S. R.; Suslick, K. S. *Inorg. Chem.* **2003**, *42*, 7719−7721.

(17) (a) Benndorf, P.; Schmitt, S.; Köppe, R.; Oña-Burgos, P.; Scheurer, A.; Meyer, K.; Roesky, P. W. *Angew. Chem., Int. Ed.* **2012**, *51*, 5006−5010. (b) Jiang, H.-L.; Tsumori, N.; Xu, Q. *Inorg. Chem.* **2010**, *49*, 10001−10006. (c) Wang, H.; Liu, S.-J.; Tian, D.; Jia, J.-M.; Hu, T.-L. *Cryst. Growth Des.* **2012**, *12*, 3263−3270.
(18) (a) Binnemans, K. *Chem. Rev.* **2009**, *109*, 4283−4374. (b) Moore, E. G.; Samuel, A. P. S.; Raymond, K. N. *Acc. Chem. Res.* **2009**, *42*, 542−552.
(19) (a) Tanner, P. A.; Duan, C.-K. *Coord. Chem. Rev.* **2010**, *254*, 3026−3029. (b) Gawryszewska, P.; Sokolnicki, J.; Legendziewicz, J. *Coord. Chem. Rev.* **2005**, *249*, 2489−2509. (c) Matthes, P. R.; Nitsch, J.; Kuzmanoski, A.; Feldmann, C.; Steffen, A.; Marder, T. B.; Müller-Buschbaum, K. *Chem.—Eur. J.* **2013**, *19*, 17369−17378.
(20) Zhou, Y.; Li, X.; Zhang, L.; Guo, Y.; Shi, Z. *Inorg. Chem.* **2014**, *53*, 3362−3370.
(21) (a) Wu, P.; Wang, J.; He, C.; Zhang, X.; Wang, Y.; Liu, T.; Duan, C. *Adv. Funct. Mater.* **2012**, *22*, 1698−1703. (b) Song, X.-Z.; Song, S.-Y.; Zhao, S.-N.; Hao, Z.-M.; Zhu, M.; Meng, X.; Wu, L.-L.; Zhang, H.-J. *Adv. Funct. Mater.* **2014**, *24*, 4034−4041. (c) Dang, S.; Min, X.; Yang, W.; Yi, F.-Y.; You, H.; Sun, Z.-M. *Chem.—Eur. J.* **2013**, *19*, 17172−17179. (d) Tang, Q.; Liu, S.; Liu, Y.; Miao, J.; Li, S.; Zhang, L.; Shi, Z.; Zheng, Z. *Inorg. Chem.* **2013**, *52*, 2799−2801. (e) Zhou, J.-M.; Shi, W.; Xu, N.; Cheng, P. *Inorg. Chem.* **2013**, *52*, 8082−8090. (f) Wu, J.-J.; Ye, Y.-X.; Qiu, Y.-Y.; Qiao, Z.-P.; Cao, M.-L.; Ye, B.-H. *Inorg. Chem.* **2013**, *52*, 6450−6456. (g) Hao, Z.; Song, X.; Zhu, M.; Meng, X.; Zhao, S.; Su, S.; Yang, W.; Song, S.; Zhang, H. *J. Mater. Chem. A* **2013**, *1*, 11043−11050.
(22) (a) He, G.; Guo, D.; He, C.; Zhang, X.; Zhao, X.; Duan, C. *Angew. Chem., Int. Ed.* **2009**, *48*, 6132−6135. (b) Falcaro, M.; Furukawa, S. *Angew. Chem., Int. Ed.* **2012**, *51*, 8431−8433. (c) Rybak, J.-C.; Hailmann, M.; Matthes, P. R.; Zurawski, A.; Nitsch, J.; Steffen, A.; Heck, J. G.; Feldmann, C.; Götzendörfer, S.; Meinhardt, J.; Sextl, G.; Kohlmann, H.; Sedlmaier, S. J.; Schnick, W.; Müller-Buschbaum, K. *J. Am. Chem. Soc.* **2013**, *135*, 6896−6902.
(23) (a) Zhu, M.; Hao, Z.-M.; Song, X.-Z.; Meng, X.; Zhao, S.-N.; Song, S.-Y.; Zhang, H.-J. *Chem. Commun.* **2014**, *50*, 1912−1914. (b) Hao, Z.; Yang, G.; Song, X.; Zhu, M.; Meng, X.; Zhao, S.; Song, S.; Zhang, H. *J. Mater. Chem. A* **2014**, *2*, 237−244. (c) Colodrero, R. M. P.; Papathanasiou, K. E.; Stavgianoudaki, N.; Olivera-Pastor, P.; Losilla, E. R.; Aranda, M. A. G.; León-Reina, L.; Sanz, J.; Sobrados, I.; Choquesillo-Lazarte, D.; García-Ruiz, J. M.; Atienzar, P.; Rey, F.; Demadis, K. D.; Cabeza, A. *Chem. Mater.* **2012**, *24*, 3780−3792.
(24) (a) Gai, S.; Li, C.; Yang, P.; Lin, J. *Chem. Rev.* **2014**, *114*, 2343−2389. (b) Heffern, M. C.; Matosziuk, L. M.; Meade, T. J. *Chem. Rev.* **2014**, *114*, 4496−4539.
(25) (a) Xue, D.-X.; Cairns, A. J.; Belmabkhout, Y.; Wojtas, L.; Liu, Y.; Alkordi, M. H.; Eddaoudi, M. *J. Am. Chem. Soc.* **2013**, *135*, 7660−7667. (b) Cui, Y.; Zou, W.; Song, R.; Yu, J.; Zhang, W.; Yang, Y.; Qian, G. *Chem. Commun.* **2014**, *50*, 719−721. (c) Hou, Y.-L.; Cheng, R.-R.; Xiong, G.; Cui, J.-Z.; Zhao, B. *Dalton Trans.* **2014**, *43*, 1814−1820. (d) Dang, S.; Zhang, J.-H.; Sun, Z.-M.; Zhang, H. *Chem. Commun.* **2012**, *48*, 11139−11141. (e) Randell, N. M.; Anwar, M. U.; Drover, M. W.; Dawe, L. N.; Thompson, L. K. *Inorg. Chem.* **2013**, *52*, 6731−6742. (f) Ma, S.; Yuan, D.; Wang, X.-S.; Zhou, H.-C. *Inorg. Chem.* **2009**, *48*, 2072−2077.
(26) (a) Wong, K.-L.; Law, G.-L.; Yang, Y.-Y.; Wong, W.-T. *Adv. Mater.* **2006**, *18*, 1051−1054. (b) Chen, Z.; Sun, Y.; Zhang, L.; Sun, D.; Liu, F.; Meng, Q.; Wang, R.; Sun, D. *Chem. Commun.* **2013**, *49*, 11557−11559. (c) Zhu, Y.-M.; Zeng, C.-H.; Chu, T.-S.; Wang, H.-M.; Yang, Y.-Y.; Tong, Y.-X.; Su, C.-Y.; Wong, W.-T. *J. Mater. Chem. A* **2013**, *1*, 11312−11319. (d) Li, H.; Shi, W.; Zhao, K.; Niu, Z.; Li, H.; Cheng, P. *Chem.—Eur. J.* **2013**, *19*, 3358−3365. (e) Dou, Z.; Yu, J.; Cui, Y.; Yang, Y.; Wang, Z.; Yang, D.; Qian, G. *J. Am. Chem. Soc.* **2014**, *136*, 5527−5530. (f) Dang, S.; Ma, E.; Sun, Z.-M.; Zhang, H. *J. Mater. Chem.* **2012**, *22*, 16920−16926. (g) Dang, S.; Zhang, J.-H.; Sun, Z.-M. *J. Mater. Chem.* **2012**, *22*, 8868−8873.
(27) (a) Chen, B.; Yang, Y.; Zapata, F.; Lin, G.; Qian, G.; Lobkovsky, E. B. *Adv. Mater.* **2007**, *19*, 1693−1696. (b) Chen, B.; Wang, L.; Xiao, Y.; Fronczek, F. R.; Xue, M.; Cui, Y.; Qian, G. *Angew. Chem., Int. Ed.* **2009**, *48*, 500−503. (c) Chen, B.; Wang, L.; Zapata, F.; Qian, G.; Lobkovsky, E. B. *J. Am. Chem. Soc.* **2008**, *130*, 6718−6719. (d) Xiao, Y.; Cui, Y.; Zheng, Q.; Xiang, S.; Qian, G.; Chen, B. *Chem. Commun.* **2010**, *46*, 5503−5505. (e) Harbuzaru, B. V.; Corma, A.; Rey, F.; Atienzar, P.; Jordá, J. L.; García, H.; Ananias, D.; Carlos, L. D.; Rocha, J. *Angew. Chem., Int. Ed.* **2008**, *47*, 1080−1083. (f) Liu, W.; Jiao, T.; Li, Y.; Liu, Q.; Tan, M.; Wang, H.; Wang, L. *J. Am. Chem. Soc.* **2004**, *126*, 2280−2281.
(28) (a) Lan, A.; Li, K.; Wu, H.; Olson, D. H.; Emge, T. J.; Ki, W.; Hong, M.; Li, J. *Angew. Chem., Int. Ed.* **2009**, *48*, 2334−2338. (b) Pramanik, S.; Zheng, C.; Zhang, X.; Emge, T. J.; Li, J. *J. Am. Chem. Soc.* **2011**, *133*, 4153−4155. (c) Pramanik, S.; Hu, Z.; Zhang, X.; Zheng, C.; Kelly, S.; Li, J. *Chem.—Eur. J.* **2013**, *19*, 15964−15971. (d) Nagarkar, S. S.; Joarder, B.; Chaudhari, A. K.; Mukherjee, S.; Ghosh, S. K. *Angew. Chem., Int. Ed.* **2013**, *52*, 2881−2885. (e) Chaudhari, A. K.; Nagarkar, S. S.; Joarder, B.; Ghosh, S. K. *Cryst. Growth Des.* **2013**, *13*, 3716−3721. (f) Germain, M. E.; Knapp, M. J. *J. Am. Chem. Soc.* **2008**, *130*, 5422−5423. (g) Li, L.; Zhang, S.; Xu, L.; Han, L.; Chen, Z.-N.; Luo, J. *Inorg. Chem.* **2013**, *52*, 12323−12325. (h) Kim, T. K.; Lee, J. H.; Moon, D.; Moon, H. R. *Inorg. Chem.* **2013**, *52*, 589−595.
(29) (a) Majumder, P. S.; Gupta, S. K. *Water Res.* **2003**, *37*, 4331−4336. (b) Boyd, S. A.; Sheng, G.; Teppen, B. J.; Johnston, C. T. *Environ. Sci. Technol.* **2001**, *35*, 4227−4234. (c) Cronin, M. T. D.; Gregory, B. W.; Schultz, T. W. *Chem. Res. Toxicol.* **1998**, *11*, 902−908.
(30) Zhang, S.-R.; Du, D.-Y.; Qin, J.-S.; Bao, S.-J.; Li, S.-L.; He, W.-W.; Lan, Y.-Q.; Shen, P.; Su, Z.-M. *Chem.—Eur. J.* **2014**, *20*, 3589−3594.
(31) (a) Sheldrick, G. M. *SHELXS-97, Programs for X-ray Crystal Structure Solution*; University of Göttingen: Göttingen, Germany, 1997. (b) Sheldrick, G. M. *SHELXL-97, Programs for X-ray Crystal Structure Refinement*; University of Göttingen: Göttingen, Germany, 1997. (c) Farrugia, L. J. *WINGX, A Windows Program for Crystal Structure Analysis*; University of Glasgow: Glasgow, UK, 1988.
(32) (a) Sun, Y.-Q.; Zhang, J.; Chen, Y.-M.; Yang, G. Y. *Angew. Chem., Int. Ed.* **2005**, *44*, 5814−5817. (b) Cheng, J.-W.; Zheng, S.-T.; Yang, G.-Y. *Dalton Trans.* **2007**, 4059−4066.
(33) Zhang, S.-R.; Du, D.-Y.; Tan, K.; Qin, J.-S.; Dong, H.-Q.; Li, S.-L.; He, W.-W.; Lan, Y.-Q.; Shen, P.; Su, Z.-M. *Chem.—Eur. J.* **2013**, *19*, 11279−11286.
(34) (a) Lan, Y.-Q.; Jiang, H.-L.; Li, S.-L.; Xu, Q. *Inorg. Chem.* **2012**, *51*, 7484−7491. (b) Liu, H.-S.; Lan, Y.-Q.; Li, S.-L. *Cryst. Growth Des.* **2010**, *10*, 5221−5226. (c) Qin, J.-S.; Zhang, S.-R.; Du, D.-Y.; Shen, P.; Bao, S.-J.; Lan, Y.-Q.; Su, Z.-M. *Chem.—Eur. J.* **2014**, *20*, 5625−5630.
(35) (a) Sørensen, T. J.; Tropiano, M.; Blackburn, O. A.; Tilney, J. A.; Kenwright, A. M.; Faulkner, S. *Chem. Commun.* **2013**, *49*, 783−785. (b) Wang, X. M.; Fan, R. Q.; Qiang, L. S.; Li, W. Q.; Wang, P.; Zhang, H. J.; Yang, Y. L. *Chem. Commun.* **2014**, *50*, 5023−5026. (c) Natur, F. L.; Calvez, G.; Daiguebonne, C.; Guillou, O.; Bernot, K.; Ledoux, J.; Pollès, L. L.; Roiland, C. *Inorg. Chem.* **2013**, *52*, 6720−6730. (d) Makhinson, B.; Duncan, A. K.; Elam, A. R.; Bettencourt-Dias, A. de; Medley, C. D.; Smith, J. E.; Werner, E. J. *Inorg. Chem.* **2013**, *52*, 6311−6318. (e) Tang, Q.; Liu, S.; Liu, Y.; He, D.; Miao, J.; Wang, X.; Ji, Y.; Zheng, Z. *Inorg. Chem.* **2014**, *53*, 289−293. (f) Gao, C.; Kirillov, A. M.; Dou, W.; Tang, X.; Liu, L.; Yan, X.; Xie, Y.; Zang, P.; Liu, W.; Tang, Y. *Inorg. Chem.* **2014**, *53*, 935−942. (g) Li, L.; Zhang, S.; Han, L.; Sun, Z.; Luo, J.; Hong, M. *Cryst. Growth Des.* **2013**, *13*, 106−110. (h) He, H.; Sun, F.; Borjigin, T.; Zhao, N.; Zhu, G. *Dalton Trans.* **2014**, *43*, 3716−3721.
(36) (a) Richardson, F. S. *Chem. Rev.* **1982**, *82*, 541−552. (b) Shi, J.; Hou, Y.; Chu, W.; Shi, X.; Gu, H.; Wang, B.; Sun, Z. *Inorg. Chem.* **2013**, *52*, 5013−5022. (c) Zhou, Y.; Guo, Y.; Xu, S.; Zhang, L.; Ahmad, W.; Shi, Z. *Inorg. Chem.* **2013**, *52*, 6338−6345. (d) Ma, X.; Li, X.; Cha, Y.-E.; Jin, L.-P. *Cryst. Growth Des.* **2012**, *12*, 5227−5232.
(37) (a) Xu, H.; Liu, F.; Cui, Y.; Chen, B.; Qian, G. *Chem. Commun.* **2011**, *47*, 3153−3155. (b) Zhang, Z.; Xiang, S.; Rao, X.; Zheng, Q.; Fronczek, F. R.; Qian, G.; Chen, B. *Chem. Commun.* **2010**, *46*, 7205−7207. (c) Guo, M.; Sun, Z.-M. *J. Mater. Chem.* **2012**, *22*, 15939−15946. (d) Tian, D.; Li, Y.; Chen, R.-Y.; Chang, Z.; Wang, G.-Y.; Bu,

X.-H. *J. Mater. Chem. A* **2014**, *2*, 1465−1470. (e) Qin, J.-S.; Bao, S.-J.; Li, P.; Xie, W.; Du, D.-Y.; Zhao, L.; Lan, Y.-Q.; Su, Z.-M. *Chem.—Asian J.* **2014**, *9*, 749−753. (f) Wang, H.; Yang, W.; Sun, Z.-M. *Chem.—Asian J.* **2013**, *8*, 982−989. (g) Wang, G.-Y.; Yang, L.-L.; Li, Y.; Song, H.; Ruan, W.-J.; Chang, Z.; Bu, X.-H. *Dalton Trans.* **2013**, *42*, 12865−12868.

(38) Gole, B.; Bar, A. K.; Mukherjee, P. S. *Chem. Commun.* **2011**, *47*, 12137−12139.

(39) (a) Salinas, Y.; Martínez-Máñez, R.; Marcos, M. D.; Sancenón, F.; Costero, A. M.; Parra, M.; Gil, S. *Chem. Soc. Rev.* **2012**, *41*, 1261−1296. (b) Sohn, H.; Sailor, M. J.; Magde, D.; Trogler, W. C. *J. Am. Chem. Soc.* **2003**, *125*, 3821−3830. (c) Zhao, D.; Swager, T. M. *Macromolecules* **2005**, *38*, 9377−9384. (d) Wu, W.; Ye, S.; Yu, G.; Liu, Y.; Qin, J.; Li, Z. *Macromol. Rapid Commun.* **2012**, *33*, 164−171. (e) Zhang, Q.; Geng, A.; Zhang, H.; Hu, F.; Lu, Z.-H.; Sun, D.; Wei, X.; Ma, C. *Chem.—Eur. J.* **2014**, *20*, 4885−4890. (f) Zhou, X.-H.; Li, L.; Li, H.-H.; Li, A.; Yang, T.; Huang, W. *Dalton Trans.* **2013**, *42*, 12403−12409.

(40) (a) Gong, Y.-N.; Jiang, L.; Lu, T.-B. *Chem. Commun.* **2013**, *49*, 11113−11115. (b) Zhang, C.; Che, Y.; Zhang, Z.; Yang, X.; Zang, L. *Chem. Commun.* **2011**, *47*, 2336−2338.